14th IEA Heat Pump Conference
15-18 May 2023, Chicago, Illinois

Design methodology of vapor compression heat pump module in Smart Thermal Energy Design platform

Bong Seong Oh[a], Gilbong Lee[a], Bongsu Choi[a], Hyungki Shin[a], Young-Jin Baik[a], Beomjoon Lee[a], Jongjae Cho[a], Gyunchul Hur[a], Sun Ik Na[a], Ho-Sang Ra[a], Eunseok Wang[a], Min Soo Kim[b], Junhyun Cho[a,*],

[a]Korea Institute of Energy Research, Gajeong-ro 152, Yuseong-gu, Daejeon, 34129, Republic of Korea

Abstract

A design platform, namely Smart Thermal Energy Design Platform (STED platform), for thermal energy-intensive industrial facilities is being developed for any user with an intuitive interface and smart guide during design process. Among design modules in STED platform, the vapor compression heat pump design module gives suitable design results for heat pumps under the given operation conditions. The module can model three heat pump layouts: basic, internal heat exchanger, and injection. To validate the design results from the module, a lab-scale heat pump experimental device, namely heat pump simulator, was made based on the calculation results from the heat pump design module. As a result, the calculated performance from the platform and the measured performance from the simulator had an error of 0.1% in terms of mean COP for 30minutes.

Keywords: Heat pump design algorithm, Internal Heat Exchanger, Injection, Design validation;

1. Introduction

According to the global energy-related CO_2 emissions by sector from IEA data [1], industry sector occupies 23% of total global CO_2 emissions. In 2021, the sector accounted for 38% (169EJ) of total global final energy use, and the fraction of fossil fuel energy in the whole industry sector final energy use was about 68% [2]. To reduce the emissions in the sector, fossil fuel based thermal systems like boilers should be electrified. Reported by Net Zero Roadmap [3], electricity share in light industry should be 76% to accomplish net zero until 2050. Heat pumps could be a great option to electrify the industrial heat because compared to electric heaters heat pumps can generate a few times of generate process heat by inputting a same electric power. Many previous works reported that energy consumption in the industrial sector could be saved about 40 to 60% if process heat under 200℃ that is utilized in most industrial sectors is replaced with heat pumps [4] [5] [6] [7] [8]. Despite these benefits of heat pumps, there is a lack of holistic design algorithms for heat pump systems because they involve various combinations of design parameters, such as cycle layouts, specifications of sub-components, refrigerants, and degrees of superheating and subcooling, and so on [9]. Thus, it is hard for small-, and medium-sized enterprises to design their own heat pump systems because they generally have deficient R&D infrastructure and insufficient capital to pay the license fees of state-of-the-art design platforms to enhance the performance of heat pumps. According to Meng et al. [10], these enterprises approximately accounted for 50% of CO_2 emissions, so that improving the performance of heat pumps used by small-, and medium-sized companies could contribute to reduction of CO_2 emissions in industry sector. To solve the problem, the latest national R&D technologies should be efficiently disseminated to those enterprises.

Smart Thermal Energy Design platform, namely STED platform could be a solution to provide preliminary design results of the thermal energy-intensive facilities such as burners, furnaces, dryers, heat exchangers, and

* Corresponding author. Tel.: +82-42-860-3581;
E-mail address: jhcho@kier.re.kr.

heat pumps to the energy consumers or vendors. Among variety of design modules, heat pump design module could treat three kinds of heat pump layouts which are basic, internal heat exchanger, and injection. In this study, the design algorithms of the layouts were suggested, and the design result of basic layout were validated with experimental test loop for heat pump design module, namely heat pump simulator.

2. Design algorithms for various heat pump layouts

At the first step to design heat pump cycle, inputs are applied into specifications of major components in a heat pump system should be inputted as listed in Table 1.

Table 1. Input list for heat pump design

Category	Input parameters	Symbol
Inputs of hot process (condenser)		
	Mass flow rate	$\dot{m}_h$
	Pressure	P_h
	Inlet temperature	T_{hi}
	Outlet temperature	T_{ho}
Inputs of cold process (evaporator)		
	Mass flow rate	$\dot{m}_c$
	Pressure	P_c
	Inlet temperature	T_{ci}
	Outlet temperature	T_{co}
Inputs of major components		
Basic cycle input *Commonly used in other layouts	Approach temperature (Plate type HX)	ΔT_{pp}
	LMTD (Fin type HX)	ΔT_{lmtd}
	Pressure drop in HX channels	ΔP
	Degree of superheat	ΔT_{sh}
	Degree of subcooling	ΔT_{sc}
	Isentropic efficiency of compressor	η_{comp}
IHX cycle input	Internal HX effectiveness	ε_{IHX}
Injection cycle	Isentropic efficiency of 2nd compressor	$\eta_{comp,2}$

The heat pump design module adopts CoolProp database for utilizing fluid properties [11], but not all fluids are not considered a refrigerant in a heat pump users intend to design owing to the computational resource problem. Instead, the appropriate refrigerants are dynamically selected from the list according to the temperature of process fluid, and the specifications of an evaporator and condenser like approach temperature and LMTD. In the condenser, a refrigerant with high pressure is condensed by the hot-side process fluid such that the critical temperature of the refrigerant is higher than the temperature of the hot-side process fluid considering the pinch point, as shown in Eq.(1). In the evaporator, a refrigerant with low pressure is evaporated by the cold-side process fluid. The refrigerant pressure in the evaporator should be higher than the ambient pressure because of the purity problem in the heat pump system. Thus, the saturation temperature of the ambient pressure considering the pinch point should be lower than that of the cold-side process fluid, as expressed in Eq.(2).

$$T_{crit} > T_{ho} + \triangle T_{pp,cond} \quad (1)$$

$$T_{NBP} < T_{co} + \triangle T_{pp,evap} \quad (2)$$

This is because heat pumps designed by the module should be a subcritical vapor compression heat pump.

2.1. Basic layout

A heat pump system with basic layout is composed of an evaporator, compressor, condenser, and expansion valve. Initially, low pressure and high pressure of the refrigerant in evaporator should be estimated considering atmosphere pressure, critical pressure, and process temperatures. The saturation temperature in evaporator can be calculated from the estimated low pressure by CoolProp database. Adding the superheat inputted by a user to the saturation temperature, the evaporator outlet temperature (i.e. compressor inlet) can be obtained. From the pressure ratio of estimated high to low pressure, and the entered isentropic efficiency of a compressor, the compressor outlet state (i.e. condenser inlet) can be calculated as shown in Eq.(3)(4).

$$T_{comp\_in} = T_{sat@P_{evap}} + \Delta T_{sh} \tag{3}$$

$$h_{comp\_out} = \left(1 - \frac{1}{\eta_{comp}}\right) h_{comp\_in} + \frac{h_{comp\_out\_ideal}}{\eta_{comp}} \tag{4}$$

The saturation temperature in condenser can be calculated from the assumed high pressure of refrigerant in condenser, and the condenser outlet temperature can be obtained by subtracting degree of subcooling from the saturation temperature in condenser as written in Eq.(5). After condenser inlet and outlet temperature are defined, mass flow rate of the system can be calculated by energy conservation between refrigerant side and process fluid side as shown in Eq.(6)(7). The subscripts 'hot_in,sec' and 'hot_out,sec' mean the inlet and outlet state of hot secondary flow like water and air in condenser. However, the approach temperature point in condenser does not usually exist at the channel inlet or outlet as single-phase heat exchangers do. This is because phase change occurs on refrigerant side in condenser while do not happened in process fluid side. To search the approach temperature in channels, the condenser channel should be divided into finite discrete nodes, and each state can be obtained based on energy conservation equation as shown in Figure. 1. Comparing the calculated approach temperature of condenser to the approach temperature inputted by a user, the error can be defined as Eq.(8). If the error is not met under the entered tolerance, the high pressure in condenser is adjusted until satisfying the convergence tolerance.

$$T_{cond\_out} = T_{sat@P_{cond}} - \Delta T_{sc} \tag{5}$$

$$Q_{cond} = \dot{m}_{hot,sec}(h_{hot\_out,sec} - h_{hot\_in,sec}) \tag{6}$$

$$\dot{m}_{ref} = Q_{cond}/(h_{cond\_in} - h_{cond\_out}) \tag{7}$$

$$\varepsilon > \left|\Delta T_{pp,cond} - \Delta \hat{T}_{pp,cond}\right| \tag{8}$$

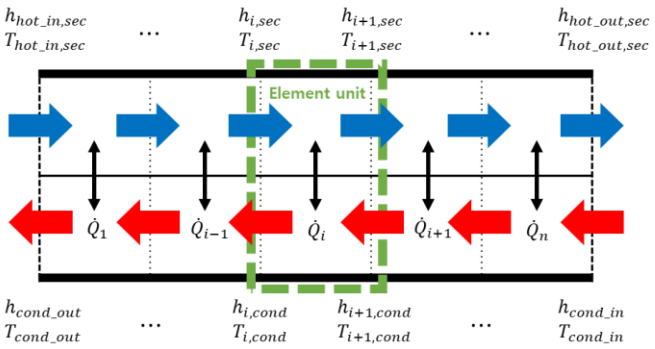

Figure. 1. Internal channel calculation of condenser using finite discrete nodes

After the condenser outlet state is obtained, through expansion valve, evaporator inlet state can be calculated through with isenthalpic process of the condenser outlet state to the low pressure as expressed in Eq,(9).

$$T_{evap\_in} = f(P_{evap}, h_{cond,out}) \tag{9}$$

Thus, evaporator inlet and outlet can be determined, and the approach temperature of evaporator is also calculated by the finite discrete nodes method similar to the condenser as shown in Eq.(10)(11)(12). The subscripts 'cold_in,sec' and 'cold_out,sec' mean the inlet and outlet state of cold secondary flow like water and air in evaporator. The error of evaporator's approach temperature is a criterion to judge the convergence of low pressure in evaporator.

$$Q_{evap} = \dot{m}_{ref}\left(h_{evap\_out} - h_{evap\,in}\right) \tag{10}$$

$$h_{cold\_out,sec} = h_{cold\_in,sec} - Q_{evap}/\dot{m}_{cold,sec} \tag{11}$$

$$\varepsilon > \left|\Delta T_{pp,set} - \Delta T_{pp,evap}\right| \tag{12}$$

When both the approach temperature errors of condenser and evaporator are under the user inputted tolerance,

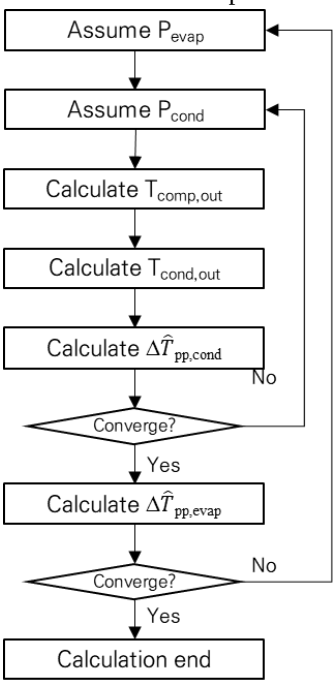

the cycle design is completed. Figure.2 shows the flow chart for designing a basic layout heat pump.

2.2. Internal heat exchanger layout

The design algorithm of IHX heat pump is basically identical with that of the basic layout heat pump but the evaporator outlet and condenser outlet transfer their heat through IHX, so the superheat at the compressor inlet and subcooling at the expansion inlet is more enhanced by the IHX. In the IHX channels, the phases of condenser and evaporator are both single phase. Therefore, the transferred heat can be calculated based on the effectiveness of IHX inputted by a user. Eq.(13) to (18) show the calculation process of IHX cold side and hot side states.

$$T_{\mathrm{IHX}\_ci} = T_{sat@P_{evap}} + \Delta T_{sh} \tag{13}$$

$$T_{\mathrm{IHX}\_hi} = T_{sat@P_{evap}} - \Delta T_{sc} \tag{14}$$

$$q_{\mathrm{ideal}} = \min\left(h_{\mathrm{IHX}\_hi} - h_{\mathrm{IHX}\_ho}^{ideal},\ h_{\mathrm{IHX}\_co}^{ideal} - h_{\mathrm{IHX}\_ci}\right) \tag{15}$$

$$q_{actual} = \varepsilon_{IHX} q_{\mathrm{ideal}} \tag{16}$$

$$h_{IHX\_co} = h_{IHX\_ci} + q_{actual} \tag{17}$$

Figure.2. Design algorithm of basic layout heat pump

$$h_{IHX\_ho} = h_{IHX\_hi} - q_{actual} \tag{18}$$

Figure.3 shows the design algorithm of a IHX layout heat pump.

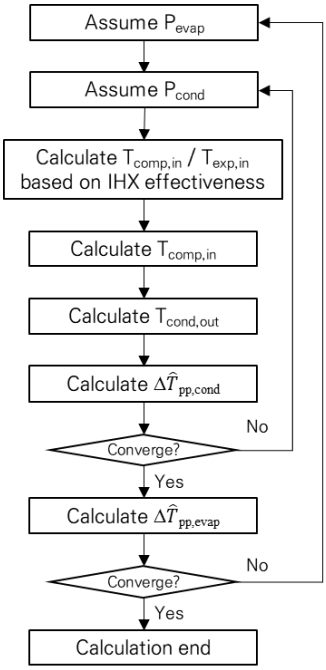

Figure.3. Design algorithm of IHX layout heat pump

2.3. Injection layout

An injection layout heat pump does not directly expand from the high pressure at condenser to the low pressure at evaporator, but there is a flash tank with intermediate pressure between condenser and evaporator. Thus, when the high pressure fluid expands in flash tank, the subcooled refrigerant at the condenser outlet changes saturated state, so that saturation gas partly appears in the tank in Eq.(19). Bypassing the gas to the middle of compression process in a compressor, consumption work of the compressor is substantially decreased due to the intercooling of the compression process in Eq.(20). Remarkably, as intermediate pressure changes, the injection layout heat pump has optimal performance point as illustrated in Figure.4.

$$x_{fsh} = f(P_{inter}, h_{cond\_out}) \tag{19}$$

$$h_{comp2\_in} = x_{fsh} h_{fsh\_v} + (1 - x_{fsh}) h_{comp1\_out} \tag{20}$$

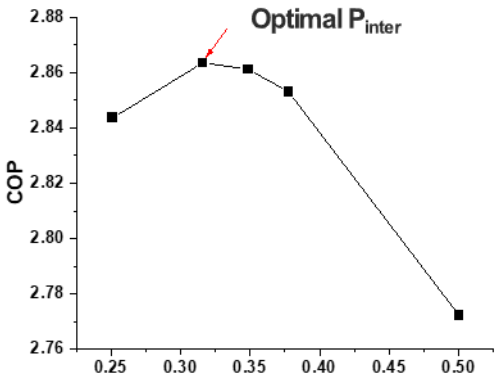

Figure.4. Optimal intermediate pressure for maximal COP

Figure.5 shows the flow chart of injection layout heat pump.

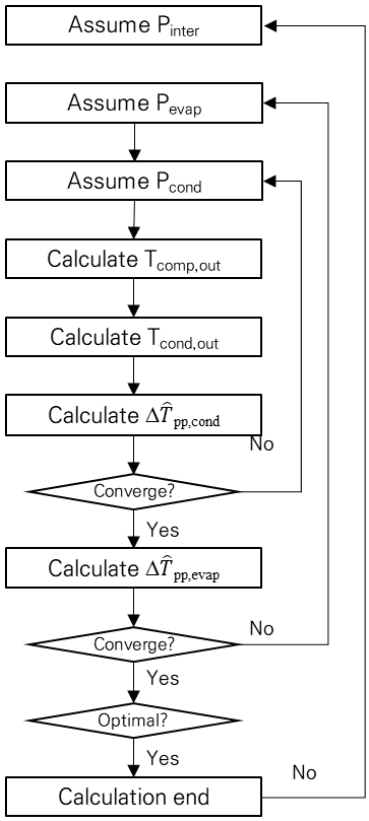

Figure.5. Design algorithm of injection layout heat pump

3. Heat pump simulator

To validate the calculation results from the heat pump design module in STED platform, a simulator was built. The simulator is composed of a compressor, plate type condenser and evaporator, and EEV. The compressor is a twin rotary (two cylinder rolling piston type) with hermetic motor, and PVE oil. Temperatures are measured by RTD with 1/16-inch probe, and pressures of compressor inlet and outlet are measured by high accuracy pressure transmitter with FS ±0.075%. Coriolis flow meter is adopted to obtain the mass flow rate in the system. Figure.5 shows the picture of simulator for heat pump design module in STED platform.

Figure.6. Picture of simulator for heat pump design module in STED platform

The monitoring system of the simulator was implemented by Labview 2020 version. The heat pump design platform was embedded in the Labview, so that the platform results and measurements directly compared on the monitoring system. In Figure.7, the center PFD shows the schematic flow lines of the simulator, and the left side the comparison results of platform calculation and measurements. Especially, the cycle states can be expressed by TS and PH diagrams, and the blue line represents the platform results and red lines shows the measurements from the simulator. They show high agreement between platform and simulator. Moreover, calculating the COPs calculated from the platform and measured from the simulator, the estimated error was only 0.1% with average of 30 minutes. Table 2 shows the differences of major parameters between calculation from the platform and measurements from the simulator. Due to the measurement error of power meter, the compression work showed the largest deviation. Coincidently, the measurement of evaporation heat is also smaller than the calculation so that COP has extremely low error. The difference of subcooling is not reported because the condenser outlet of refrigerant side is in the saturated state so that it is hard to compare the calculation of subcooling to the measurement.

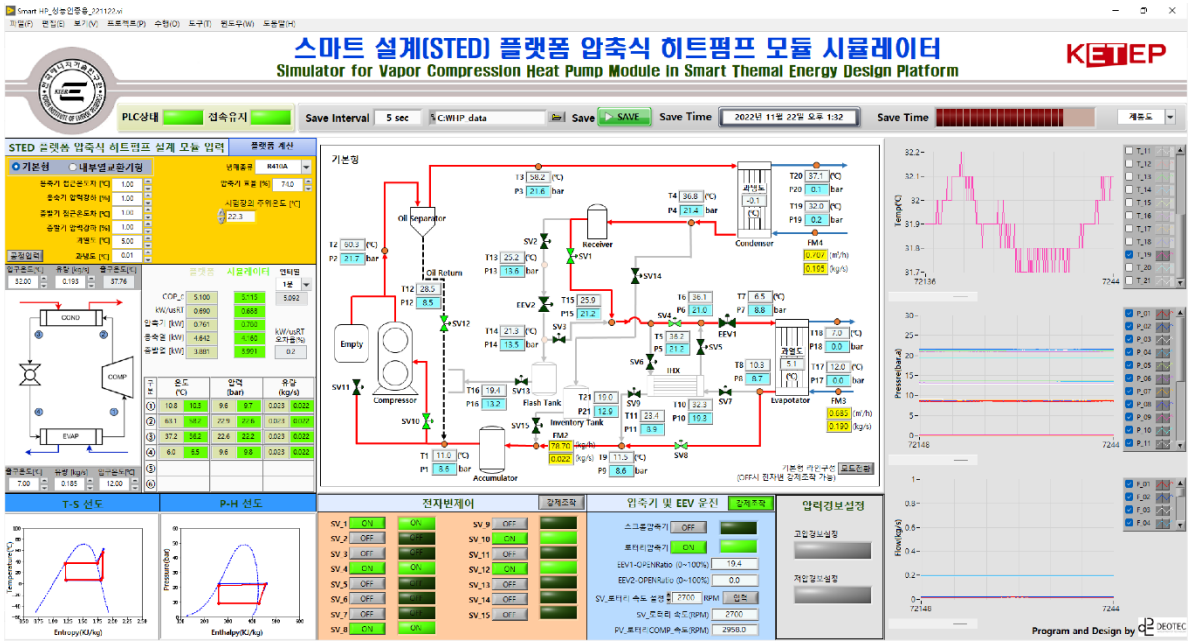

Figure.7. The monitoring system of the simulator

Table 2. Absolute errors between calculation results and measurements

Parameters	Calculation results	Measurements	Differences [%]
COP	5.1	5.093	0.14
Evaporation heat	3.89 kW	4.05 kW	4%
Compression work	0.761 kW	0.795 kW	4.4%
Evaporating pressure	9.6 bar	9.68 bar	0.8%
Condensing pressure	22.9 bar	22.5 bar	1.9%
Superheat	5 ℃	5.17 ℃	3.5%

4. GUI of heat pump design module

After the results of the heat pump design module was demonstrated, the platform was visualized by PyQt5 module in Python library. The first step is selecting heat pump layout a user wants to design. At the next step, the user enter the required inputs as listed in Table 1. Finishing the calculation, the results are summarized with the refrigerant states, and essential diagrams.

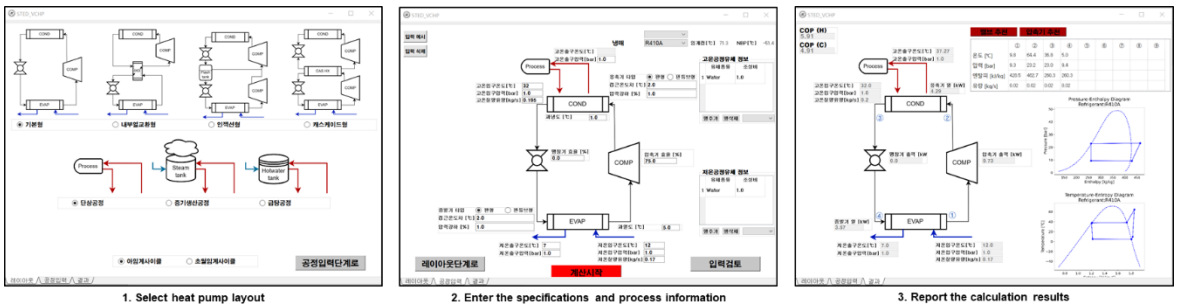

Figure.8. GUI manual

5. Results

To respond to demands for developing user-friendly design platform, Smart Thermal Energy Design platform was developed. Among the thermal energy-intensive facilities the platform treats, the heat pump module algorithms were discussed in this study. Basic, internal heat exchanger, and injection cycles are dealt with, and basic layout heat pump was validated by the simulator with mean error of 0.1%. Thus, the heat pump design module in the platform can provide accurate design results to users.

Acknowledgements

This work was supported by the Korea Institute of Energy Technology Evaluation and Planning (KETEP) and the Ministry of Trade, Industry & Energy (MOTIE) of the Republic of Korea (No. 20202020800200, Development and demonstration of smart design platform technology for thermal energy-instensive industrial facilities).

References

[1] "IEA, Global energy-related CO2 emissions by sector, IEA, Paris." https://www.iea.org/data-and-statistics/charts/global-energy-related-co2-emissions-by-sector, IEA. Licence: CC BY 4.0.

[2] "IEA, Final energy consumption by fuel in the Net Zero Scenario, 2000-2030, IEA, Paris." https://www.iea.org/data-and-statistics/charts/final-energy-consumption-by-fuel-in-the-net-zero-scenario-2000-2030, IEA. Licence: CC BY 4.0.

[3] S. Bouckaert *et al.*, "Net Zero by 2050: A Roadmap for the Global Energy Sector," 2021.

[4] A. K. Jana and A. Mane, "Heat Pump Assisted Reactive Distillation: Wide Boiling Mixture," *AIChE J.*, vol. 57, no. 11, 2011, doi: 10.1002/aic.12518.

[5] M. Yang, X. Feng, and G. Liu, "Heat integration of heat pump assisted distillation into the overall process," *Appl. Energy*, vol. 162, pp. 1–10, 2016, doi: 10.1016/j.apenergy.2015.10.044.

[6] S. Singh and M. S. Dasgupta, "CO2 heat pump for waste heat recovery and utilization in dairy industry with ammonia based refrigeration," *Int. J. Refrig.*, vol. 78, pp. 108–120, 2017, doi: 10.1016/j.ijrefrig.2017.03.009.

[7] Y. Liu, E. A. Groll, K. Yazawa, and O. Kurtulus, "Energy-saving performance and economics of CO2 and NH3 heat pumps with simultaneous cooling and heating applications in food processing: Case studies," *Int. J. Refrig.*, vol. 73, pp. 111–124, 2017, doi: 10.1016/j.ijrefrig.2016.09.014.

[8] B. Zühlsdorf, F. Bühler, R. Mancini, S. Cignitti, and Brian Elmegaard, "High Temperature Heat Pump Integration using Zeotropic Working Fluids for Spray Drying Facilities," *Proc. 12th IEA Heat pump Conf.*, no. July, pp. 1–11, 2017.

[9] J. F. Horn and P. H. Scharf, "Design Considerations for Heat Pump Compressors," *Int. Compress.*

Eng. Conf. Sch., pp. 194–201, 1976.

[10] B. Meng *et al.*, "More than half of China's CO2 emissions are from micro, small and medium-sized enterprises," *Appl. Energy*, vol. 230, no. September, pp. 712–725, 2018, doi: 10.1016/j.apenergy.2018.08.107.

[11] I. H. Bell, J. Wronski, S. Quoilin, and V. Lemort, "Pure and Pseudo-pure Fluid Thermophysical Property Evaluation and the Open-Source Thermophysical Property Library CoolProp," *Ind. Eng. Chem. Res.*, vol. 53, no. 6, pp. 2498–2508, Feb. 2014, doi: 10.1021/ie4033999.